Scaled Radar Cross Section Measurements with Terahertz-Spectroscopy up to 800 GHz

C. Jansen[#1], N. Krumbholz[#2], R.Geise[*3], A. Enders[*4], M. Koch[#5]

[#] *Institut für Hochfrequenztechnik, TU Braunschweig, Germany*

[1]christian.jansen@ihf.tu-bs.de

[*] *Institut für Elektromagnetische Verträglichkeit, TU Braunschweig, Germany*

[3]r.geise@tu-bs.de

***Abstract*—Radar cross section measurements of complex, large objects (e.g. aircraft) are usually performed on miniaturized models, as this enables a well controllable measurement environment. The system frequency in the scaled scenario is proportional to the inverse size ratio of the model compared to the original object. If a high scaling factor is required to accommodate the measurement setup in a laboratory, the scaled frequencies can reach several hundred gigahertz, hardly accessible with today's network analyzers, especially when high frequency radar applications are concerned. Consequently, this paper discusses the feasibility and accuracy of terahertz spectroscopy, which allows accessing the frequency range of up to and even above 1 THz, for such measurements. In this initial study, radar cross section measurements of a perfectly conducting sphere and a metal plate are in good agreement with the theory up to 800 GHz, demonstrating the capability of the measurement setup.**

I. Introduction

Radar cross section (RCS) measurements are an established method for obtaining characteristic object information, required for target identification. Especially when large, complex geometries, such as aircraft, are considered, scaled setups are commonly employed. In these setups, the measurement frequency is increased by the same factor that the object size is reduced, so that their relation remains unchanged. As typical radars operate at frequencies of several gigahertz (GHz), scaling factors of one hundred and higher lead to frequencies of several hundred GHz in the laboratory setup. Scaled RCS measurements of an aircraft, using a network analyzer have been performed up to 310 GHz in [1]. Furthermore, measurements in the W-band between 75 to 110 GHz have been presented [2]. For even higher frequencies, most network analyzer concepts reach their technological limits.

In [3], Cheville et al. demonstrated the feasibility of terahertz time domain spectroscopy measurements in the context of impulse ranging studies by qualitatively comparing the scattered field amplitude of a 1/200th scale model MiG-29 and a 1/200th scale model F-117A ''Stealth'' fighter aircraft in the time domain for a monostatic measurement setup. The diminishing of the field in case of the stealth aircraft in contrast to the strong response of the MiG-29 was clearly visible. However, no RCS or angle dependent analysis was given in this work.

Here, we suggest the use of a fiber coupled terahertz time domain spectroscopy setup for scaled RCS studies with measuring frequencies extending from 100 GHz to above 1 THz.

II. Experimental Setup

The measurement setup is depicted in Fig. 1. Fiber coupled terahertz receiver and transmitter heads are mounted on two movable rails in a bistatic configuration. The transmitter and receiver consist of photoconducting dipole antennas on a GaAs substrate and are optically gated by fs-laser pulses generated by a titan-sapphire laser. Two high density polyethylene (HDPE) lenses with a diameter of 5.08 cm and a focal length of f = 60 mm are employed to collimate the terahertz beam. The sampled THz time domain pulses are Fourier transformed in a postprocessing step. For automation of the measurement process, a step motor is used for varying the angle between transmitter and receiver. For more information on the fiber coupled spectrometer setup, the inclined reader is referred to reference [4], were a detailed description can be found.

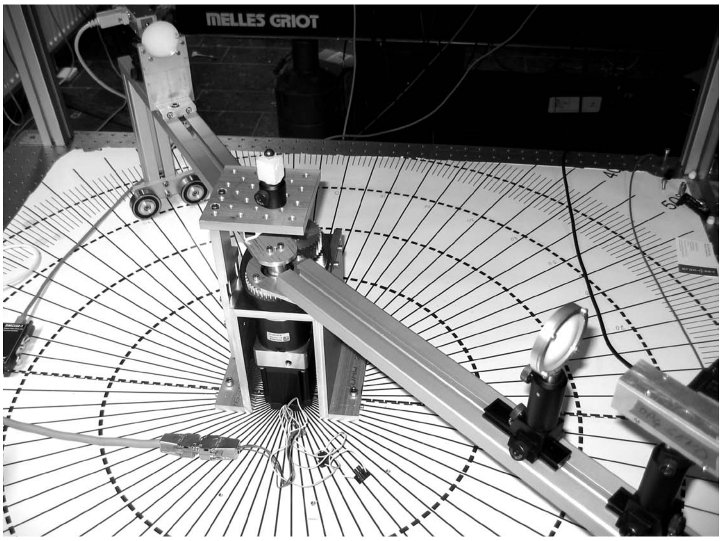

Fig. 1 Layout of a fiber coupled terahertz time domain spectroscopy setup for bistatic scaled RCS measurements

The object of interest is positioned in the centre of the setup on a polystyrene foam pillow. This material is especially suited, as it exhibits a refractive index close to that of air and negligible absorption, so that the scattering characteristics of the investigated objects remain mostly unchanged.

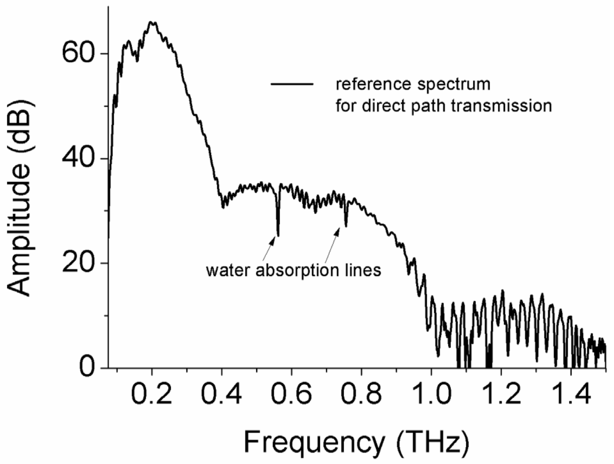

Fig. 2 Reference spectrum of the fibre coupled THz time domain spectrometer

As shown in Fig. 2, the system bandwidth is 1 THz for the direct line of sight link without any scattering object in the beam path. The spectrum reveals two domains: A high power section beneath 0.4 THz, where the dipole characteristic of the photoconductive antennas enhances the emission, and a lower power section above 0.4 THz, where the emission is governed by the photocarrier dynamics. While the first domain has a clear maximum at 0.25 THz, decreasing rapidly to lower and higher frequencies, the second domain has a relatively flat spectral response, slowly decreasing towards shorter wavelengths. At 0.55 THz and 0.74 THz, water absorption lines are present so that these frequencies should be avoided for the RCS evaluation.

III. FREQUENCY DOMAIN RCS

The common RCS formulation in the frequency domain [5] is given by:

$$\sigma(\Phi_{in},\Phi_{obs}) = S_{21scattered}{}^{2} \cdot (4\pi\, r_1\, r_2)^2 \cdot \frac{4\pi}{\lambda^2} \cdot \frac{1}{G_e G_r}, \quad (1)$$

with:

σ	radar cross section
$S_{21scattered}$	ratio between scattered and incident field
Φ_{in}	angle of incidence
Φ_{out}	observation angle
r_1, r_2	distances from antennas to target
G_e,G_r	antenna gains
λ	wavelength

To obtain the frequency dependent product of both antenna gains as required for (1) as well as the path loss, a direct line of sight measurement (Φ_{in} = 180°, Φ_{out} = 0°) without any scattering object has been conducted. The scattered transfer function $S_{21scattered}$ was determined by vectorial subtraction of a reference spectrum, measured without any object in the beam path and a sample spectrum with the scattering object present for each investigated observation angle Φ_{out}. Thus, in contrast to measurements with a vector network analyzer, the terahertz time domain spectroscopy measurements are inherently calibration free.

IV. MEASUREMENTS OF A METALLIC SPHERE

To characterize the accuracy of the measurement setup, objects with a well identified RCS are examined. The first is a metallic sphere with a diameter of 1 cm. An analytical RCS calculation can be found in [6]. As the maximum RCS of a sphere is at the direct forward scatter direction, this measurement scenario is well suited for the investigation in a bistatic setup. The sphere was measured with transmitter position fixed at 180° in one half-plane and the receiver position varied in the opposed half-plane as shown in Fig. 3.

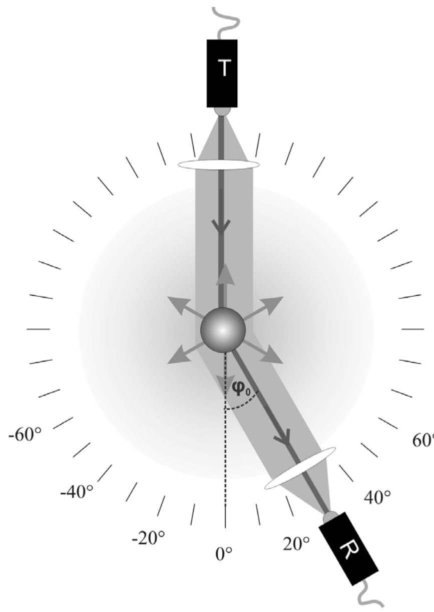

Fig. 3 Setup employed for RCS measurements on a metallic sphere

Fig. 4 and Fig. 5 present the corresponding simulations and measurements for the bistatic RCS of a 1 cm diameter metallic sphere at 300 GHz and 800 GHz, respectively. The simulated RCS profile is accurately reproduced in the measured results. In case of the 300 GHz measurement, the positions of the side lobes as well as the amplitude of the scattered field agree well with the predicted values and deviations from the analytically calculated RCS results are typically less than 3 dB.

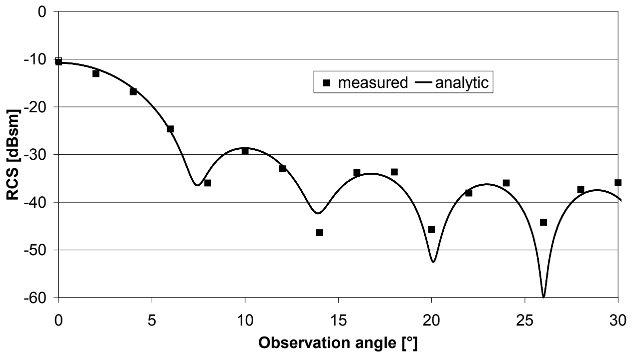

Fig. 4 Simulated and measured RCS of a 1 cm diameter metallic sphere at 300 GHz

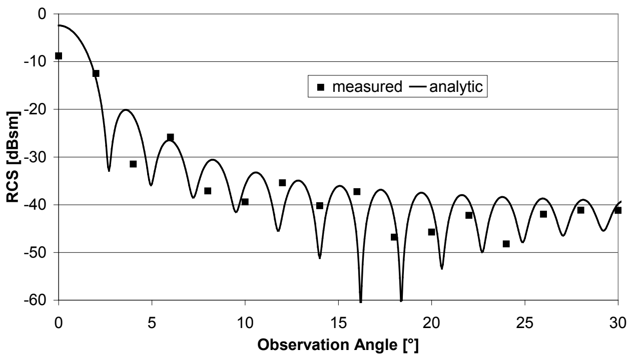

Fig. 5 Simulated and measured RCS of a 1 cm diameter metallic sphere at 800 GHz

In case of the 800 GHz measurement, the strength of the scattered field is also well reproduced, but the angle resolution of 2° is too low to sample single local minima and maxima at this frequency. Improving the angular resolution is likely to lead to even better results.

V. Measurements with a Metallic Plate

In addition to RCS measurements of a metallic sphere, we also present measurements of a small (15 mm x 15 mm) metallic plate. The maximum RCS of a plate is in the specular direction. This also allows the evaluation of the setup in a quasi monostatic scenario for small angles of incidence. While the RCS of the sphere is analytically calculable, the RCS analysis of metal plates requires an approximated solution, e.g. the high-frequency prediction technique of the physical optics (PO) method [7]. The PO approximation is valid if the dimensions of the metal plate are much larger than the wavelength and if both the incident and the observation angle are not too far off to the broadside direction of the plate. In case of the metallic plate measurements, both the transmitter and the receiver share the same half-plane. While the transmitter remains at a fixed position the receiver position is varied. Fig. 6 shows a sketch of the measurement setup with the coordinate system as well as the field and the wave vectors.

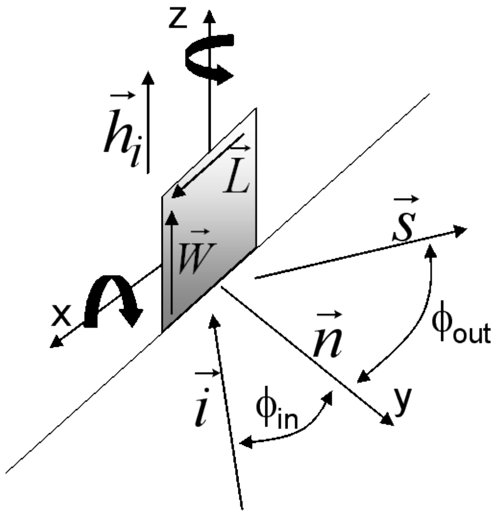

Fig. 6 Sketch of the measurement geometry with marked field and wave vectors for the RCS analysis of the metallic plate

In case of the metallic plate, the degrees of freedom for misalignment angles around the x-axis and z-axis have to be considered, which are negligible in case of the metallic sphere due to its complete symmetry.

The measurements are performed at an incidence angle ϕ_{in} of 35°. The measured scattering profile encompasses observation angles ϕ_{out} of ±12° around the specular direction. For this geometry the prediction of the radar cross section σ according to the physical optics approach [7] is obtained by the equation:

$$\sqrt{\sigma(\vec{i},\vec{s})} = \frac{k|\vec{L}||\vec{W}|\vec{n}\vec{s}}{\sqrt{\pi}} \frac{\sin\left[\frac{1}{2}k\vec{L}(\vec{i}-\vec{s})\right]}{\left[\frac{1}{2}k\vec{L}(\vec{i}-\vec{s})\right]} \frac{\sin\left[\frac{1}{2}k\vec{W}(\vec{i}-\vec{s})\right]}{\left[\frac{1}{2}k\vec{W}(\vec{i}-\vec{s})\right]}, \quad (3)$$

with :
$\vec{L}$: longitudinal orientation and length of the plate ,
$\vec{W}$: lateral orientation and width of the plate,
$\vec{i}$: direction of incident wave,
$\vec{s}$: direction of the scattered wave,
$\vec{n}$: normal vector of the plate.

The post-processing procedure of the experiment data is the same as discussed above for the case of the metallic sphere. From a direct transmission measurement the antenna gains are obtained and applied to the RCS equation. Simulations using the PO method are calculated for a perfectly aligned measurement setup. Additionally, simulations considering a slight misalignment are also shown. For the best agreement of simulations and measurements, a tilt angle of 0.3° around the

z-axis and -1.3° around the x-axis has to be assumed, which lies within the expected accuracy of the sample mount. It is planned to improve the setup in the future by inserting optical alignment components to compensate any sample tilt.

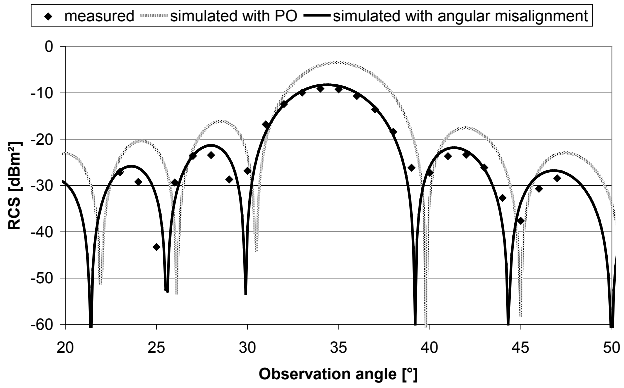

Fig. 7 Simulated and measured RCS for a metallic plate with 1.5 cm x 1.5 cm side lengths at 300 GHz

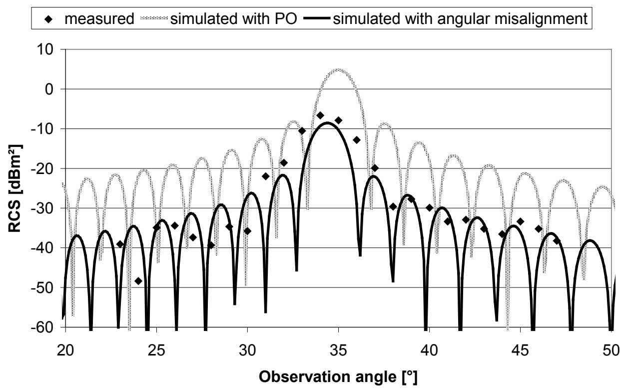

Fig. 8 Simulated and measured RCS for a metallic plate with 1.5 cm x 1.5 cm side lengths at 800 GHz

Fig. 7 shows the results of the simulations and the measurements for the RCS at 300 GHz. An excellent agreement between the measurement and the PO simulations both with respect to the qualitative profile as well as the absolute RCS values is achieved.

The envelope of the scattering profile at 800 GHz, shown in Fig. 8, also agrees well between simulations and measurements, but the measured profile does not reflect all the simulated features due to the limited angle resolution of 1°. However, both measurements show the high potential of the calibration-free THz time domain spectroscopy technique for scaled RCS measurements.

VI. Conclusion and Outlook

In this paper, we demonstrated the feasibility of terahertz time domain spectroscopy for scaled RCS measurements at frequencies in the range between 300 and 800 GHz. The RCS of a metallic sphere and a metallic plate were analyzed both with simulations and experimentally obtained RCS data to evaluate the accuracy of the proposed technique. The good agreement between the measurements and simulations both in case of the sphere and the plate clearly demonstrate the feasibility of scaled THz RCS studies in monostatic and bistatic configuration.

Future work will improve the system bandwidth, enabling RCS measurements at even higher frequencies. Additionally, optical components used for highly accurate sample alignment will further improve the data quality. Furthermore, measurements with a higher angle resolution will enable the reproduction of sharp features in the RCS profile down to the limit set by the receiver's antenna pattern.

To conclude, terahertz time domain spectroscopy systems could also be employed to access the frequency regime above 1 THz, enabling scaled RCS measurements for high frequency radars, even when high model scaling factors are required.

References

[1] A. Lönnqvist et al., "*Phase-Hologram-Based Compact RCS Test Range at 310 GHz for Scale Models*", IEEE Transactions on Microwave Theory and Techniques, Vol. 54, June 2006, pp 2391-2397.

[2] R.Geise et al., "*Feasibility Study on Scaled Bistatic RCS Measurements of Aircraft in W-Band to Investigate Misguidance by the Instrument-Landing-System*", IEEE AP-S Int. Symp., July. 2008, San Diego.

[3] R.A. Cheville et al., "*Time Domain Terahertz impulse ranging study*", Appl. Phys. Lett., vol. 67, No. 14, pp. 1960–1962, Oct. 1995.

[4] N. Vieweg et al., „*Fiber-coupled THz spectroscopy for monitoring polymeric compounding processes*",Proc. of the SPIE Europ. Symp. on Opt. Metr., vol. 6616, pp. 66163, 2007

[5] C.A. Balanis, *"Antenna Theory, Analysis and Design"*, John Wiley & Sons, Inc. 1997, pp.88-90.

[6] F. Knott, Radar Cross Section, Artech House Inc., 1985, pp. 88-90.

[7] F. Knott, Radar Cross Section, Artech House Inc., 1985, pp.119-130.